Theoretical and experimental investigation of the nonlinear dynamics of nanobubbles excited at clinically relevant ultrasound frequencies and pressures: the role of lipid shell buckling

Amin JafariSojahrood[1,2], Lenitza Nieves[3], Christopher Hernandez[4], Agata Exner[3], Michael C. Kolios[1,2]

[1]Physics, Ryerson University, Toronto, ON, Canada, [2]Institute for Biomedical Engineering, Science and Technology (iBEST), partnership between St. Michael's Hospital and Ryerson University, Toronto, ON, Canada, [3]Radiology, Case Western Reserve University, Cleveland, Ohio, USA, [4]Biomedical Engineering, Case Western Reserve University, Cleveland, Ohio, USA, 5Institute for Biomedical Engineering, Science and Technology (iBEST), a partnership between St. Michael's Hospital and Ryerson University, Toronto, ON, Canada

Abstract—The usage of microbubbles (MBs) is limited to the blood pool due to their large size yet the detection of biomarkers on tumor cells and effective drug delivery, require MBs to reach the tumor tissue outside of the vasculature. To tackle these problems, nanobubbles (NBs) are proposed as a potential alternative. NBs can pass through submicron blood vessels and extravasate to tissue. Due to their higher number density; higher doses of NBs can be delivered to the target. However, despite their potential, the use of NBs has been limited because of the limited information of their complex dynamics. In this work, we manufactured lipid and surfactant-stabilized C3F8 NBs (mean diameter ~200 nm). NB scattering response was investigated by single bubble scattering experiments with narrowband pulses with 16-55 MHz and acoustic pressure of 0.250-1.5 MPa (Vevo-770 Machine,Fujifilm visualsonics), and in-vivo imaging at 18 MHz and 4% power (Vevo 3100, Fujifilmvisualsonics). The nonlinear response of the NBs was numerically studied by solving the Marmottant model for the US pulses used in the experiments. The results were visualized using the resonance curves and bifurcation diagrams of the oscillations of the NBs versus frequency and pressure. Experimental results demonstrate strong echogenicity of NBs at a frequency range of 10-25 MHz. Single NB experiments suggest that NBs generate strong subharmonic and super harmonic responses even at lower acoustic pressures ~250 kPa. This contradicts the linear theoretical predictions, as the resonance frequency (fr) of the NBs is calculated to be ~130 MHz. Results of numerical simulations show that when the initial surface tension of the NBs is ~<0.01 N/m, the fr of the NBs rapidly decreases as the acoustic pressure increases. Thus, NBs become active at frequencies below 50 MHz due to the nonlinear behavior of the lipid shell. Bifurcation diagrams confirmed the generation of subharmonics and super harmonics only for NBs which are initially close to the buckling state.

I. Introduction

Microbubbles (MBs) excited by ultrasound are used as contrast agents for the detection of blood vessels. They can also be used to enhance drug delivery [1]. Due to their relatively large size, the application of MBs is limited to the blood pool; however, the detection of biomarkers on tumor cells and effective drug delivery, requires that the MBs reach the tumor tissue outside of the vasculature.

To provide a solution to this problem, nanobubbles (NBs) are proposed as a plausible substitute [2-5]. NBs can pass through submicron blood vessels and extravasate to the tissue. Additionally, because of their larger number density, higher doses of NBs can be delivered to the target. NBs have recently been successfully applied to enhance the detection of the tumor tissue in small animal imaging [2-5].

Despite the broad potential applications of NBs, limited information of their complex dynamics is currently available. Recent observations [2-5] demonstrate strong echogenicity of the NBs within the frequency range 10-25 MHz. The strong echogenicity of the NBs is contrary to the predictions of the linear theory for the resonant oscillations of the NBs.

Knowledge on the nonlinear dynamics of the NBs will help in better optimization of the imaging and therapeutic applications of NBs. In order to have better understanding on the complex dynamics of NBs, and to shed light on the apparent contradiction between the linear theory and experimental observations, the oscillatory behavior of NBs (with 200-700 nm diameter) was studied both experimentally and numerically.

II. Methods

A. Numerical methods

To numerically investigate the oscillations of the NBs, the Marmattont [6] model was used to investigate the dynamics of the NBs:

$$\rho_l\left(R\ddot{R}+\frac{3}{2}\dot{R}^2\right)=\left[P_0+\frac{2\sigma(R_0)}{R_0}\right]\left(\frac{R}{R_0}\right)^{-3\gamma}\left(1-\frac{3\dot{\gamma}}{c}\dot{R}\right)-\frac{2\sigma(R)}{R}-\frac{4\eta_l\dot{R}}{R}-\frac{4\kappa_s\dot{R}}{R^2}-P_0-P_{ac}(t), \quad (1)$$

where R_0 is the initial radius, ρ_L is the density of the liquid, P_0 is the equilibrium pressure inside the bubble, Γ is the polytropic exponent, μ_L is the viscosity of the surrounding liquid, μ_L is the liquid viscosity, κ_s is the surface dilatational viscosity of the shell, and $\sigma(R)$ is the initial surface tension which is given by equation 2:

$$\sigma(R)=\begin{cases}0, & \text{if } R\leqslant R_{buckling}\approx R_0\\ \chi\left(R^2/R_{buckling}^2-1\right), & \text{if } R_{buckling}\leqslant R\leqslant R_{breakup}\\ \sigma_{water}=0.072\ \mathrm{N\,m^{-1}}, & \text{if } R>R_{rupture}\end{cases} \quad (2)$$

where χ is the shell elasticity and:

978-1-5386-3383-0/17/$31.00 ©2017 IEEE

$$R_b = \frac{R_0}{\sqrt{1 + \frac{o(R_0)}{\chi}}}$$

And

$$R_r = R_b \sqrt{1 + \frac{\sigma_{break-up}}{\chi}}$$

Dynamics of the NBs, were numerically simulated for a large range of the control parameters of the system (NB initial radius (R_0=100nm-300nm), surface tension (0-0.07 N/m), frequency (1-150 MHz) and pressure (1kPa-500 kPa)). The results were visualized using the resonance and bifurcation diagrams of the NBs similar to the methods described in [7-10].

B. Experiments

The lipids DBPC (1,2-dibehenoyl-sn-glycero-3-phosphocholine), DPPA (1,2 Dipalmitoyl-sn-Glycero-3-Phosphate), and DPPE (1,2-dipalmitoyl-sn-glycero-3-phosphoethanolamine) were obtained from Avanti Polar Lipids (Pelham, AL), and mPEG-DSPE (1,2-distearoyl-*sn*-glycero-3-phosphoethanolamine-N-[methoxy(polyethylene glycol)-2000] (ammonium salt)) was obtained from Laysan Lipids (Arab, AL). Pluronic L10 was donated by BASF (Shreveport, LA). Bubbles were prepared by dissolving DBPC, DPPA, DPPE and mPEG-DSPE in chloroform in a 6.15:2:1:1 mass ratio. Following solvent evaporation, the lipids were hydrated in a solution containing 50 µl of glycerol and 1 mL of phosphate buffered saline (PBS) containing 0.06 wt.% of Pluronic L10 at 80°C for 30 minutes. Once hydrated, the air inside of the vial was replaced with octafluoropropane (C_3F_8) gas. The vial was then agitated using a VialMix shaker (Bristol-Meyers Squibb Medical Imaging, N. Billerica, MA) for 45 s. Nanobubbles were isolated from the total bubble population based on their buoyancy by centrifugation at 50·*g* for 5 min. With these parameters, all bubbles larger than 0.7 µm should rise 0.5 cm or greater. Nanobubbles were isolated by collecting below this distance in the vial.

NB scattering response was investigated by attempted single bubble scattering experiments with narrowband pulses with 12.5-55 MHz and acoustic pressure of 0.250-1.5 MPa (Vevo-770 Machine, Fujifilm visualsonics) using a method similar to [10-11], and in-vivo imaging at 18 MHz,1fps, and 4% power (Vevo-3100, Fujifilm visualsonics) following tail vein injections of 100 ul of either MicroMarker (Visualsonics) or NBs. Time-intensity curves (TIC) were obtained in the same mouse for both contrast agents.

III. RESULTS

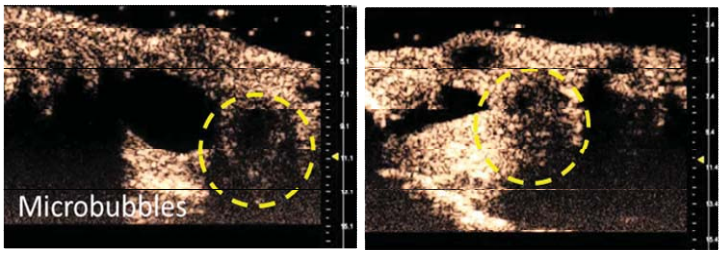

Figure 1: Contrast harmonic image of orthotopic PC3 prostate tumor in the same mouse imaged at 18 MHz using the Vevo 3100 (Fujifilmvisualsonics) Left: with microbubbles, Right: with NBs.

Figure 1 shows a sample contrast harmonic image of an orthotopic PC3 prostate tumor in mice at 18 MHz acquired after the injection of MBs (left) and NBs (right). Figure 2shows the echo power of the region of interest (the tumor) in Fig. 1. In comparison with sonication with MBs at the same injection volume (which corresponds roughly to equivalent total gas volume) the sonication with the NBs resulted in a 5 fold increase in the peak intensity.

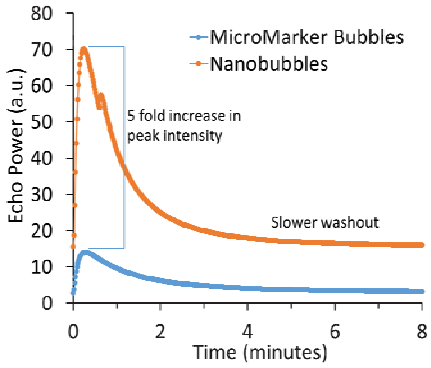

Figure 2: The Echo power versus time of the ROIs in figure 1.

To better understand the mechanism of the enhanced echogensity of the NBs, the Marmottant model was simulated for the conditions that was discussed in the previous section. Figure 3 shows the resonance curves and the radial displacement of a NB sonicated with pulses with P=10 kPa of pressure and 40 cycles durations. The resonance frequency (f_r) of the NB has one main peak and the NB with initial surface tension of 0.001 N/m has a lower fr (~80 MHz) compared to the NB with initial surface tension of 0.06 N/m (~130 MHz). As the pressure increases to 50 kPa (Fig. 4a) the main resonance peak of the NB with initial surface tension of 0.001 N/m decreases rapidly and super-harmonic resonances apear in the resonance diagram within the freqeuncy range of <50 MHz. The radial displacement of the NB with 0.001 N/m surface tension (Fig. 4b) is significantly larger than the NB with 0.06 N/m. Increasing the pressure up to 200 kPa, results in further decrease of the resonance freqeuncy of the NB with initial surface tension of 0.001 N/m. However, it did not have a significant effect on the f_r of the NB with 0.06 N/m surface tension (Fig 5a-b).

978-1-5386-3383-0/17/$31.00 ©2017 IEEE

Figure 6a-b shows the bifurcation diagarm of the R/R_0 of the NB with R0=200 nm sonicated at P=50 kPa and 200 kPa, respectively. Results demonstrate the enhanced nonlinear oscillations, including the super harmnic oscillations and subharmonic oscillations for the NB with initial surface tension of 0.001 N/m (even for freqeuncies<50 MHz), while the NB with initial surface tension of 0.06 N/m was unable to exhibit any detectable nonlinearity. Figure 7 shows the nromalized maximum backscattered intensity (the maximum backscattered intensity at each surface tensition is normalized to the maximum achivable backscattered intensity over the range of initial surface tensions that was studied) of a NB sonicated at P=200 kPa and f=12 MHz versus the initial surface tension. The maximum responses of the NB occur for the initial surface tensions below 0.01 N/m, thus NBs which are initially close to buckling state exhbit stronger echogenecity, in contrast; NBs with higher surface tension exhibit a weak response.

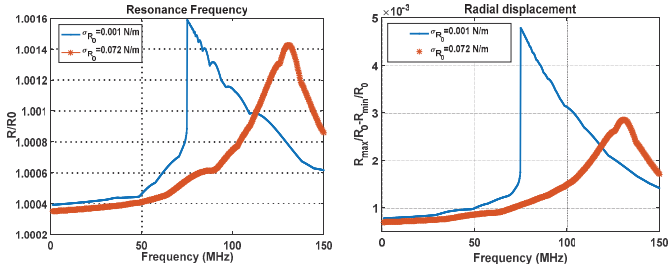

Figure 3: a) Resonance frequency (fr), and b) Radial displacement of a nano bubble R0= 200 nm, sonicated with P=10 kPa.

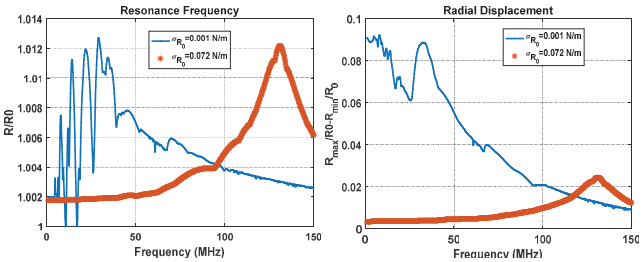

Figure 4: a) Resonance frequency (f_r), and b) Radial displacement of a nano bubble R0= 200 nm, sonicated with P=50 kPa.

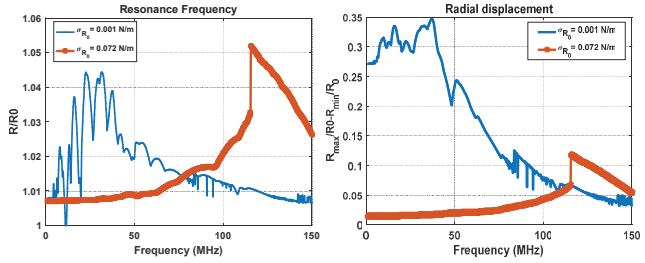

Figure 5: a) Resonance frequency (f_r), and b) Radial displacement of a nano bubble R0= 200 nm, sonicated with P=200 kPa.

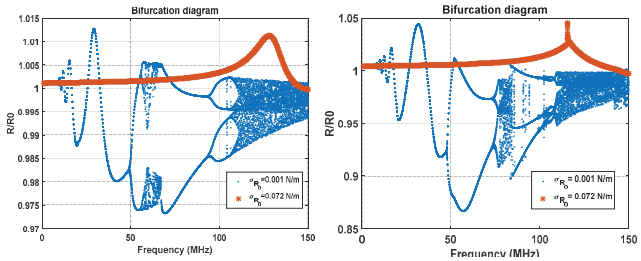

Figure 6: Bifurcation diagram of R/R_0 of the oscillations of NB with R0= 200 nm, sonicated with a) P=50 kPa and b) 200 kPa

Figure 8a-c shows 3 samples of the experimentally detected subharmonic (SH) response of what is tought to be single NBs at a) 25 MHz, b) 16 MHz and c) 12.5 MHz sonicated with pressures of ~50-250 kPa. The existense of the SH oscillations at such low pressure thresholds and high freqeuncies may be one indication that the initial surface tension of most of the NBs in our experiments were initially close to zero.

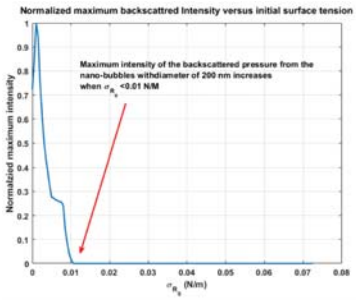

Figure 7: The normalized backscattered Intensity of a NB with a diameter of 200 nm versus the Initial surface tension.

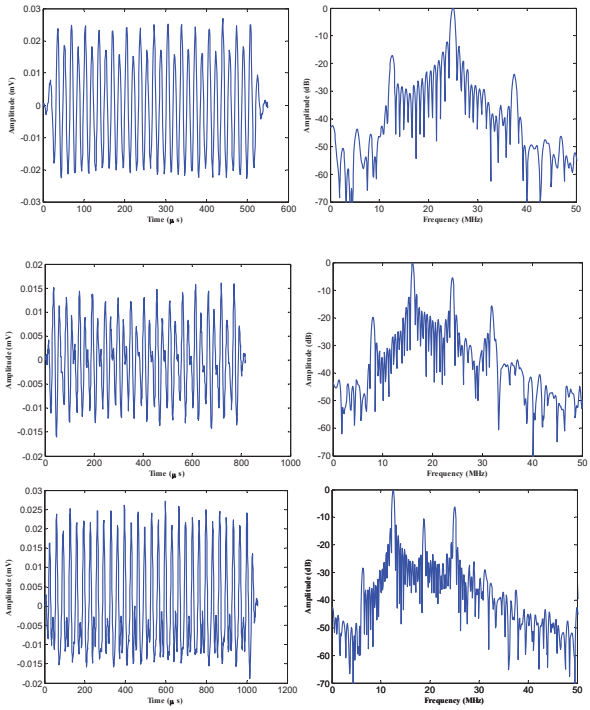

Figure 8: Experimentally detected subharmonic signals and their freqeuncy spectra of single NB events through sonication of a polydisperse dilute population of floating NBs at pressures of ~100-200 kPa when: a) f= 25 MHz, b) f= 16 MHz and c) f=12.5 MHz.

978-1-5386-3383-0/17/$31.00 ©2017 IEEE

IV. Discussion

In this work, the nonlinear dynamics of NBs were studied both experimentally and numerically. In-vivo results showed strong echogenicity of the NBs at frequencies <20 MHz. NB experiments in dilute solutions showed that NBs can generate strong subharmonic and super harmonic responses even at lower acoustic pressures ~<250 kPa and frequencies <30 MHz. This contradicts the linear theoretical predictions, as the mean resonance frequency of the NBs in our experiments, is calculated to be ~130 MHz. Results of the numerical simulations showed that when the initial surface tension of the NBs is below ~0.01 N/m the f_r of the NBs rapidly decreases as the acoustic pressure increases. This decrease, is much faster than the changes of the (f_r) with respect to pressure in the absence of the buckling [8]. Thus, one plausible hypothesis of the strong activity of NBs at frequencies below 50 MHz may be due to the buckling of the lipid shell. More in detail measurements of size and surface tension, and experimental measurements alongside with numerical simulations are needed to fully confirm this hypothesis.

Acknowledgment

This work was funded in part by the Prostate Cancer Research Program under Award No. W81XWH-l6-l-037I (to AAE). We also acknowledge additional support from the Case Comprehensive Cancer Center P30CA043703 in the form of a pilot grant. Views and opinions of, and endorsements by the author(s) do not reflect those of the National Institutes of Health or of the Department of Defense. Additionally, we acknowledge the contribution of Drs. Gopi Gopalakrishnan, Jacob Lilly and Hansheng Xia in the acquisition of *in vivo* data.

We acknowledge the additional funding by the Terry Fox and CIHR. This work is also supported by CFI funding for instrumentation.

References

[1] Ferrara, K., Pollard, R., Borden, M.: Ultrasound microbubble contrast agents: fundamentals and application to gene and drug delivery. Ann. Rev. Biomed. Eng. 9, 415–447 (2007)

[2] Gao y, et. al, Ultrasound molecular imaging of ovarian cancer with CA-125 targeted nanobubble contrast agents, Nanomedicine: NBM, 13 (2017) 2159–2168

[3] Reshani, P. H., et al., Improving performance of nanoscale ultrasound contrast agents using N,N-diethylacrylamide stabilization, Nanomedicine: NBM 2017;13:59-67

[4] Reshani, P. H., et al., Ultrasound imaging beyond the vasculature with new generation contrast agents, Wiley Interdisciplinary Reviews: Nanomedicine and Nanobiotechnology, 7 (2015) 593-608

[5] H Wu, et al., Acoustic characterization and pharmacokinetic analyses of new nanobubble ultrasound contrast agents, Ultrasound in medicine & biology 39 (11), 2137-2146

[6] Marmottant et al, A model for large amplitude oscillations of coated bubbles accounting for buckling and rupture. J AcoustSoc Am, 118 (2005), 3499–3505

[7] AJ Sojahrood, MC. Kolios, Classification of the nonlinear dynamics and bifurcation structure of ultrasound contrast agents excited at higher multiples of their resonance frequency, Phys. Lett. A, 356, (2012), 2222-2229

[8] AJ Sojahrood et al., Influence of the pressure-dependent resonance frequency on the bifurcation structure and backscattered pressure of ultrasound contrast agents: a numerical investigation, Nonlinear Dynamics, 80, (2015), 889-904

[9] S. Behnia, AJ Sojahrood, W. Soltanpoor and L. Sarkhosh, Towards classification of the bifurcation structure of a spherical cavitation bubble, Ultrasonics, 49(8), 2009, 605-610.

[10] AJ Sojahrood , R. Karshafian and MC. Kolios, Bifurcation structure of the ultrasonically excited microbubbles undergoing buckling and rupture, Proceedings of Meetings on Acoustics 19 (1), (2013), 075097

[11] O. Falou , AJ Sojahrood , J.C. Kumaradas and M.C. Kolios, Surface modes and acoustic scattering of microspheres and ultrasound contrast agents, Journal of the Acoustical Society of America, Volume 132, Issue 3, pp. 1820-1829 (2012).

978-1-5386-3383-0/17/$31.00 ©2017 IEEE